Optimal nonlinear control of an industrial emulsion polymerization reactor

I D Gil, J C Vargas, Jean Pierre Corriou

▶ **To cite this version:**

I D Gil, J C Vargas, Jean Pierre Corriou. Optimal nonlinear control of an industrial emulsion polymerization reactor. Chemical Engineering Research and Design, 2016, 10.1016/j.cherd.2016.04.016 . hal-02383501

HAL Id: hal-02383501
https://hal.science/hal-02383501v1

Submitted on 27 Nov 2019

HAL is a multi-disciplinary open access archive for the deposit and dissemination of scientific research documents, whether they are published or not. The documents may come from teaching and research institutions in France or abroad, or from public or private research centers.

L'archive ouverte pluridisciplinaire **HAL**, est destinée au dépôt et à la diffusion de documents scientifiques de niveau recherche, publiés ou non, émanant des établissements d'enseignement et de recherche français ou étrangers, des laboratoires publics ou privés.

Optimal nonlinear control of an industrial emulsion polymerization reactor

I.D. Gil[a,b], J.C. Vargas[a], J.P. Corriou[b]

[a] *Departamento de Ingeniería Química y Ambiental, Universidad Nacional de Colombia Ciudad Universitaria, Bogotá - Colombia (e-mail: idgilc@unal.edu.co)*
[b] *Laboratoire Réactions et Génie des Procédés, CNRS, Université de Lorraine, ENSIC 1, Rue Grandville, B.P. 20451, 54001, Nancy Cedex, France (e-mail: jean-pierre.corriou@univ-lorraine.fr)*

Abstract

In this paper, the modelling, dynamic optimization and nonlinear control of an industrial emulsion polymerization reactor producing poly-vinyl acetate (PVAc) are proposed. The reaction is modeled as a two-phase system composed of an aqueous phase and a particle phase according to the model described in our previous work (Gil et al., 2014). The case study corresponds to an industrial reactor operated at a chemical company in Bogotá (Colombia). An industrial scale reactor (11 m^3 of capacity) is simulated. Three different dynamic optimization problems are solved from the more simplistic (only one control variable: reactor temperature) to the more complex (three control variables: reactor temperature, initiator flow rate and monomer flow rate) in order to minimize the reaction time. The results show that it is possible to minimize the reaction time while some polymer desired qualities (conversion, molecular weight and solids content) satisfy defined constraints. The optimal temperature profile and optimal feed policies of the monomer and initiator, obtained in a dynamic optimization step, are used as optimal set points for reactor control. A nonlinear geometric controller based on input/output linearization is implemented for temperature control.

Keywords: Dynamic optimization, Nonlinear geometric control, Optimal temperature profile, Optimal feed policies, Polymerization, Vinyl acetate.

1. Introduction

The purpose of dynamic optimization studies is to determine a set of variables of a dynamic system, such as flow rates, temperatures, pressures, heat duties, ..., that optimize a given cost function or criterion (costs, productivity, time, energy, selectivity) subject to specific constraints (dynamic model, operating conditions, safety and environmental restrictions). Some of the common problems of chemical engineering addressed by means of dynamic simulation and optimization include startup, upset, shutdown and transient analysis, safety studies, control and scheduling of batch and semi-batch processes, and the validation of control schemes (Biegler, 2007; Cervantes and Biegler, 2008). In all cases, it is important to possess a dynamic model sufficiently representative of the real process by means of mass and energy balances, and algebraic equations for physical and thermodynamic relations, but with a moderate complexity in order to get a mathematical and numerical solution without difficulty (Corriou, 2004, 2012).

Some of the most important objectives in resins and polymer production plants are related to the improvement of safety, quality and productivity, minimum operating costs and respect of environmental constraints (Gentric et al., 1999). These make the optimization and control of polymerization reactors of great interest. In most cases, an optimization problem for a polymerization system requires the definition of an objective function and constraints which are defined by the reaction time and/or polymer molecular characteristics, together with operating conditions. In terms of polymerization reactors, the main contributions concern homogeneous reactions and some multiphase considerations trying to minimize the batch period, improve quality control and minimize the molecular weight distribution. In these cases, nonlinear models are essential to accurately describe the dynamics of the process. The solution of this kind of optimal control problems can be obtained by means of various optimization methods such as variational calculus, Hamilton-Jacobi equations, Pontryagin's maximum principle for continuous time systems and Bellman dynamic programming for discrete time systems, among others (Corriou, 2004, 2012; Kameswaran and Biegler, 2006; Biegler, 2007).

In the case of emulsion polymerization, several studies deal with dynamic optimization. For example, (Jang and Yang, 1989) report the dynamic minimization of the final time of a batch emulsion polymerization of vinyl acetate using initiator flow rate as control variable, and the maximum allowable reac-

tion rate together with the total amount of initiator as constraints. (Gentric et al., 1999) calculate the optimal temperature profile that minimizes the batch time of a copolymerization reactor of styrene and α-methylstyrene using orthogonal collocation coupled with a sequential quadratic programming method. As constraints, they used the final conversion and the final number average molecular weight. (Sayer et al., 2001) and (Vicente et al., 2002) calculated the optimal monomer and chain-transfer agent feed profiles for the semi-batch methylmethacrylate (MMA)/n-butylacrylate (n-BA) emulsion copolymerization, using iterative dynamic programming with an objective function that included a term for the copolymer composition and also a term for the molecular weight distribution, in a way close to multiobjective optimization. (Araújo and Giudici, 2003) used variable time intervals with an iterative dynamic programming procedure to minimize the reaction time while composition and molecular weight are controlled at specific values. (Paulen et al., 2010) worked on the dynamic optimization of the emulsion copolymerization of styrene and α-methylstyrene applying control vector parameterization (CVP) method in order to minimize the total reaction time. Recently, batch and semibatch operation of copolymerization of styrene and MMA (Ibrahim et al., 2011) were studied in order to maximize the monomer conversion in one case and the average molecular weight in a second case by means of CVP techniques solved by successive quadratic programming. Multiobjective optimization refers to simultaneous optimization of more than one objective function, which is typical in most real-life optimization problems encountered in industry (Benyahia et al., 2011). Multiobjective dynamic optimization has been also studied for a semibatch styrene polymerization process in order to establish optimal operating temperature and feeding policies, which maximize monomer conversion and minimize the residual initiator in the final product (Silva and Biscaia Jr., 2004).

In the present work, the dynamic optimization of the industrial emulsion polymerization of vinyl acetate is performed with respect to three different optimization scenarios. In the three cases, the objective is to minimize the reaction time by varying separately or simultaneously the reactor temperature, initiator flow rate and monomer flow rate. After optimization, some open loop optimal results obtained are used for comparison with closed loop simulations. The nonlinear geometric controller coupled with state estimation is used for tracking the optimal reaction temperature profile found by dynamic optimization. The results show the potential of dynamic optimization in finding optimal feed policies and operating temperature to improve

the productivity. Also, it is demonstrated that the optimal temperature trajectory is well followed by means of a nonlinear controller.

2. Dynamic optimization of vinyl acetate emulsion polymerization

2.1. Experimental validation of the model

The dynamic state space model of the process has been described in a previous work (Gil et al., 2014). Nine states are used $[I, M_t, M_M, V_{pol}, \mu_0, \mu_1, \mu_2, T, T_j]$ standing respectively for the initiator concentration I, total added monomer M_t, remaining monomer M_M, total volume of polymer V_{pol}, three first moments of polymerization μ_i, reactor temperature T and jacket temperature T_j. The first seven equations correspond to the reaction kinetics and the two following equations to the energy balances for the reactor and jacket.
Kinetic model:

$$\frac{dI}{dt} = q_I - k_I I \tag{1}$$

$$\frac{dM_t}{dt} = q_M \tag{2}$$

$$\frac{dM_M}{dt} = q_M - \mathcal{R}_{pol} \tag{3}$$

$$\frac{dV_{pol}^p}{dt} = \mathcal{R}_{pol}\frac{MW_M}{\rho_{pol}} \tag{4}$$

$$\begin{aligned}\frac{d\mu_0}{dt} = \; & \left(k_{fm}\left[M\right]^p + k_{fp}\mu_0 + k_t\lambda_0\right)\alpha\lambda_0 - \\ & k_{fp}\lambda_0\left(\mu_0 - \left(1-\alpha\right)^2\alpha\lambda_0\right) + 0.5k_t\lambda_0^2\end{aligned} \tag{5}$$

$$\begin{aligned}\frac{d\mu_1}{dt} = \; & \frac{\lambda_0}{1-\alpha}\left(\left(k_{fm}\left[M\right]^p + k_{fp}\mu_0 + k_t\lambda_0\right)\alpha\left(2-\alpha\right) + k_t\lambda_0\right) - \\ & k_{fp}\lambda_0^2\left(1-\alpha\left(1-\alpha\right)^2\right)\end{aligned} \tag{6}$$

$$\begin{aligned}\frac{d\mu_2}{dt} = \; & \frac{\lambda_0}{\left(1-\alpha\right)^2}\left(2\alpha\left(k_{fm}\left[M\right]^p + k_{fp}\mu_0 + k_t\mu_0\right) + k_t\lambda_0\left(2\alpha+1\right)\right) \\ & -2k_{fp}\lambda_0^2\left(\frac{1-\alpha\left(1-\alpha\right)^3}{1-\alpha}\right) + \frac{d\mu_1}{dt}\end{aligned} \tag{7}$$

Reactor dynamics:

$$\frac{dT}{dt} = \frac{\sum q_i C_{p,i}(T_i - T) - \Delta H_r \mathcal{R}_{pol} + UA(T_j - T) - Q_{cond}}{\sum m_i C_{p,i}} \tag{8}$$

$$\frac{dT_j}{dt} = \frac{F_j\left(T_{j_{in}} - T_j\right)}{m_w} - \frac{UA}{m_w C_{p,w}}\left(T_j - T\right) \tag{9}$$

The major part of the model has been validated previously (Araújo and Giudici, 2003; Arora et al., 2007) based on the experimental data obtained by (Penlidis et al., 1985; Penlidis, 1986). The main modifications to the model are related to the energy balances for the reactor and the jacket. In this section, a simulation of a pilot plant reactor from a Colombian chemical company is reported, in order to reproduce its industrial operation, to compare the results with some measurements of the solids content and to have an idea of the reaction conversion. Some tests in a pilot scale reactor were carried out and the results were compared with a simulation of the same system using Matlab. A semi-batch emulsion polymerization reaction of vinyl acetate was performed. The used recipe is given in Table 1. The reactor temperature was fixed taking into account the preheating step. The monomer and initiator flow rates were adjusted manually by the operator during the whole operation. The goal is to maintain a nearly constant value of the temperature in the reactor. In the current operation of the industrial reactor, a jacket is used but only for the initial preheating step. During the reaction, temperature is maintained almost constant by manipulating only initiator and monomer flow rates. Consequently, the temperature cannot accurately follow a given set point and this limits the feed flow rate of the reactants in view of a more efficient process. For that reason, a different control is desirable with efficient use of the jacket. To that intent, energy balances of the reactor will be used to take into account the behavior of the jacket and reactor contents. This will be useful in the next stages of the work to propose a control strategy associated also to a dynamic optimization of the system.

Table 1: Recipe used in the pilot emulsion polymerization reactor

Component	Load (kg)
Water	36
Vinyl acetate	35
Potassium persulfate	0.12
Polyvinyl alcohol	3.5

In order to follow the reaction, solids content and viscosity were measured by withdrawing samples at specific reaction times. The procedure established

for the determination of solids content in adhesives in the Colombian Technical Standards NTC-5003 (In Spanish, Norma Técnica Colombiana NTC-5003) was used. Viscosity was determined by following the Colombian Technical Standards NTC-5063 (In Spanish, Norma Técnica Colombiana NTC-5063).

The solids content ϕ_S is calculated theoretically by summing the weight of polymer formed and the weight of the polyvinyl alcohol and dividing it by the total weight of the latex

$$\phi_S = \frac{(M_t - M_M)MW_M + M_{PVOH}}{M_t MW_M + M_{PVOH} + \rho_w V_w} \tag{10}$$

The viscosity of the reactor contents η is calculated from the expression (11) proposed by (Chylla and Haase, 1993) that depends on the solids content and the reactor temperature. Some of the parameters of (11) were proposed by other authors (Graichen et al., 2006; Hvala et al., 2011) or fitted using experimental information from this test

$$\eta = c_0 e^{(c_1 \phi_S)} 10^{c_2 \left(\frac{a_0}{T} - c_3\right)} \tag{11}$$

where a_0, c_0, c_1, c_2 and c_3 are model parameters, and T is the reactor temperature.

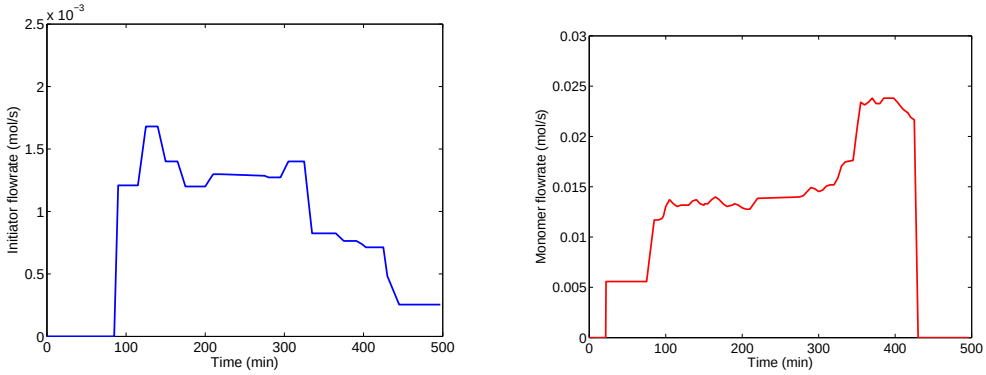

(a) (b)

Figure 1: Flow rates for the pilot reactor test. (a) Initiator, (b) Monomer

Figure 1 shows monomer and initiator flow rates used during all the reaction. As it was mentioned previously, these flow rates are imposed manually

by the operator to guarantee a nearly constant temperature in the reactor. In the same way, Figure 2a and Figure 2b show the corresponding quantities of initiator and monomer respectively remaining in the reactor.

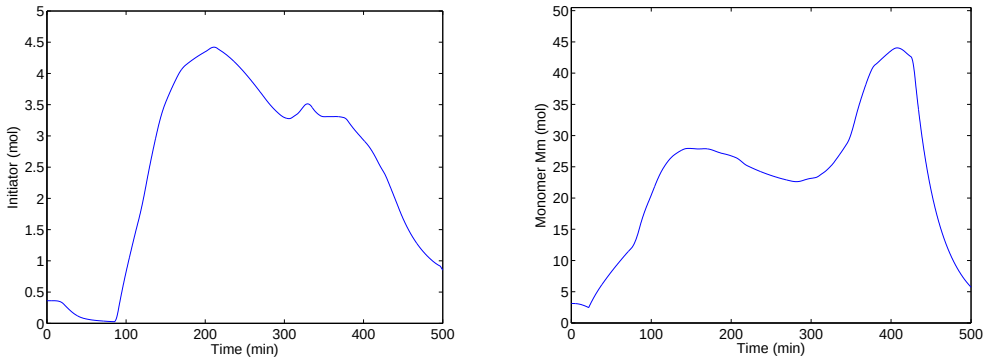

(a) (b)

Figure 2: Number of moles in the pilot reactor test. a) Initiator, b) Monomer

It can be seen that the quantity of remaining monomer in the reactor changes accordingly to variations of the monomer flow rate, and also it is influenced by additional injections of initiator that increase the polymerization rate. The initiator reacts in the first part of the batch rapidly as a result of the high increase of the temperature and then, when the initiator feed starts, there is an accumulation of initiator (Figure 2a). It is also evident that almost all the monomer is consumed in the polymerization reaction (Figure 2b) verifying the large conversions typical of emulsion polymerization processes.

Reactor temperature during the total batch time is shown in Figure 3. The average temperature in the reactor is close to 343 K. Fron Figures 2 and 3, it can be noted that, when reactor temperature increases, reaction rate also increases thus decreasing the number of moles of monomer remaining in the reactor. Average molecular weight, dispersity and conversion are presented in Figure 4. The average molecular weight and, in consequence, the dispersity are varying in function of the initiator and monomer injections during all the batch while the conversion increases up to 350 min (approx.), then decreases slowly, and finally increases until the end of the run where the conversion is higher than 98%. This is due to the effect of temperature on the reaction rate and also it can be explained by the constant initiator flow rate at the end of the batch.

Finally, in order to do a validation, simulation results of solids content

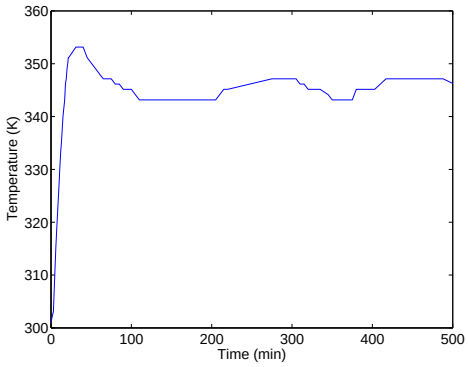

Figure 3: Temperature profile for the pilot reactor test

and viscosity were plotted with those data of experimental pilot test (Figure 5). As can be verified, there is a good representation of the solids content along the run. This is an indication of the adequacy of the model and its parameters, taking into account that the solids content is directly related to the reaction and the formation of polymer particles. On the other way, it should be noted also that, apart from a single point which is erroneous, viscosity is well represented by the model. The comparison made with the experimental data obtained shows that a good approximation with respect to typical values of viscosity of this kind of emulsions is achieved. In addition, viscosity measurement is spoilt by an experimental error that was not quantified here, but depends on the measurement technique and the operator. Of course, the experimental error has an effect on the fitting of the viscosity model to the experimental values determined in the pilot reactor.

2.2. Industrial case study

In the following, the dynamic optimization of an industrial emulsion polymerization reactor to produce poly-vinyl acetate will be presented. The case study corresponds to the industrial reactor operated in a chemical company in Colombia. An industrial scale reactor (11 m^3 of capacity) is simulated in the case where a semi-batch emulsion polymerization reaction of vinyl acetate is performed. A schematic of the reactor is shown in Figure 6. The used industrial recipe is shown in Table 2.

Three different dynamic optimization problems are solved with a piecewise constant control using different discretization scenarios. In the three problems, three different variables were considered as control variables $u(t)$:

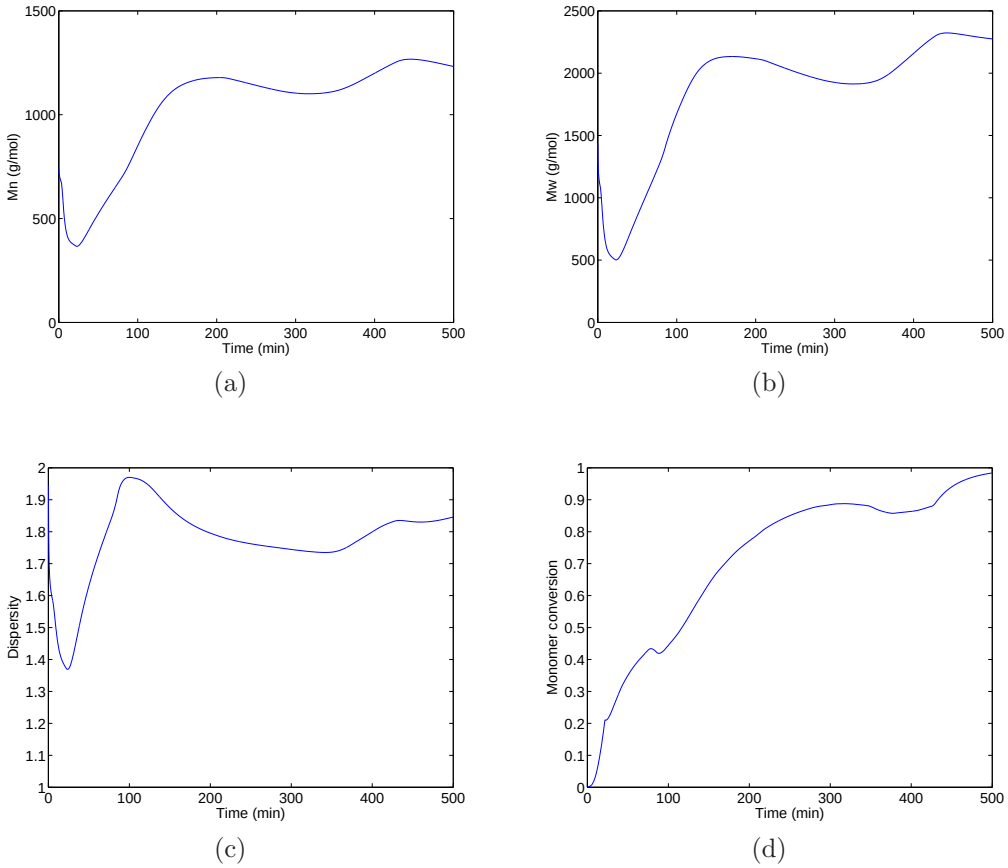

Figure 4: Quality results for the pilot reactor test. a) Number average molecular weight, b) Weight average molecular weight, c) Dispersity, d) Conversion

reactor temperature, initiator flow rate and monomer flow rate. Quality constraints are set in all the cases according to the requirements of the product and to the information provided by the company. The dynamic optimization problem is solved by means of direct optimization using the NonLinear Programmming (NLP) solver *fmincon* function in Matlab which solves constrained NLP problems. The mathematical model for the emulsion polymerization was reported in a previous work (Gil et al., 2014) and was summarized in section 2.1. In the dynamic optimization problem, the energy balances representing the reactor temperature dynamics are not considered because the reactor temperature T will be assumed as a control variable. This corresponds to an open loop control study. The model used

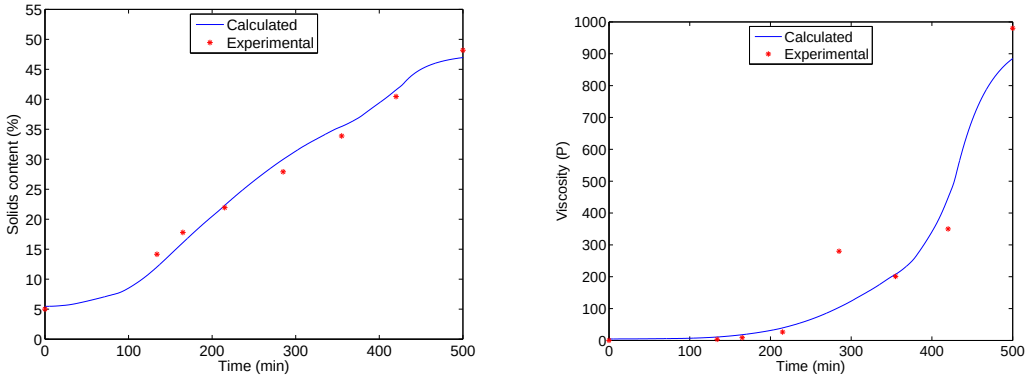

(a) (b)

Figure 5: Quality results of the experimental pilot reactor test. a) Solids content, b) Viscosity

for dynamic optimization then corresponds to the following seven states $[I, M_t, M_M, V_{pol}, \mu_0, \mu_1, \mu_2]$. Here, the goal is to calculate an optimal reactor temperature profile based on the knowledge of the polymerization kinetics. In the second part of this study, devoted to closed loop control, the dynamics of the reactor as energy balances will be considered.

2.3. Process operation

An emulsion polymerization process displays different behaviors according to the relative rates of initiation, propagation and termination, which at the same time depend on the monomer flow rate, initiator flow rate and reaction conditions. Typically, semi-batch emulsion polymerizations are divided in two steps: batch and fed-batch (Figure 7). At initial time $t = 0$, specific quantities of monomer, initiator, water and protective colloid, representing a fraction of the recipe, are charged to the reactor. In the process studied here, according to the procedure followed by the chemical company, monomer, ini-

Table 2: Recipe used for the simulation of the industrial reactor

Component	Load (kg)
Water	5400
Vinyl acetate	4651
Potassium persulfate	12.8
Polyvinyl alcohol	701

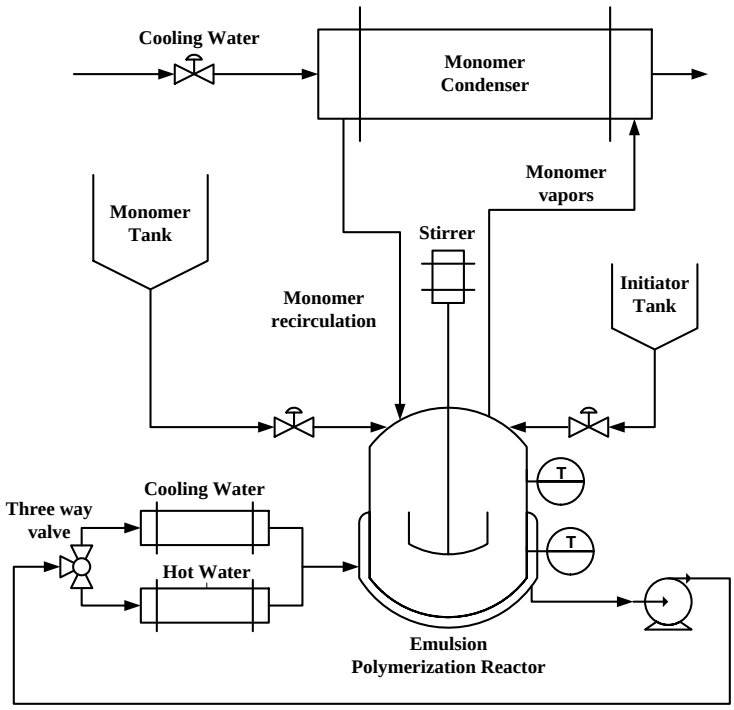

Figure 6: Schematic of the industrial emulsion polymerization reactor

tiator and protective colloid are respectively vinyl acetate, potassium persulfate and polyvinyl alcohol. A pre-heating step of the reactor is carried out by injecting steam or hot water into the reactor jacket in order to reach a temperature of 351 K. The reactor must be maintained at this temperature to ensure complete dissolution of the polyvinyl alcohol. The reaction starts when the activation temperature of the initiator is reached (approximately 340 K). This stage of the process is operated in batch mode and, during that period, primary nucleation takes place, generating most of the particles. In this stage, the total number of particles is defined and remains almost constant during the rest of the reaction, including the following fed-batch operation. The remaining monomer, according to the recipe, is fed continuously during the major part of the reactor operation (strictly speaking, during the fed-batch mode operation) and its flow rate can be adjusted to approximately regulate the reactor temperature and, in this way, partially reduce the rate of heat generation by means of its sensible heat. The initiator can be fed continuously to the reactor at a variable flow rate or, according

to the industrial procedure, by finite impulses at a constant flow rate at two or three different times during the batch. The agitation speed is constant. Because of the exothermicity of the reaction, high quantities of heat are released and the temperature inside the reactor is controlled around a specified value by adjusting the inlet jacket temperature. Three main input variables to the process can be identified, monomer flow rate, initiator flow rate and inlet jacket temperature, this latter being adjusted by means of a three way valve. The temperature is considered as a measured output. Figure 6 shows the schematic industrial reactor configuration and the main steps of a typical emulsion polymerization are summarized in Figure 7.

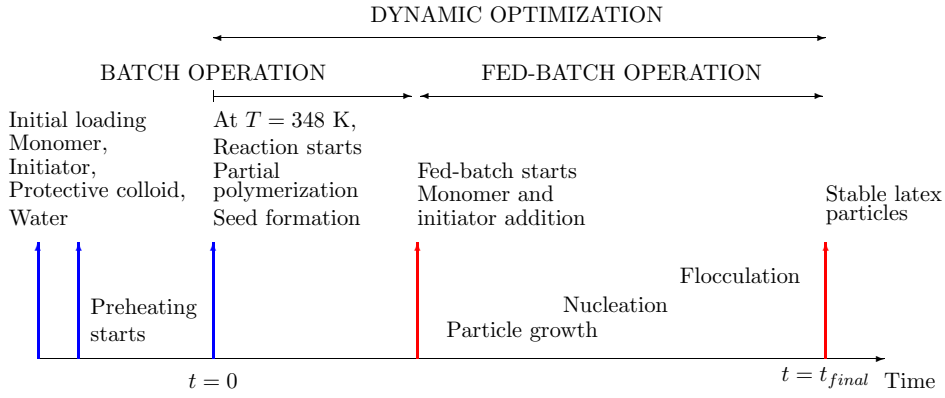

Figure 7: Sequential steps of a typical semi-batch emulsion polymerization

In this study, the pre-heating step is not taken into account for the dynamic optimization calculations. At the end of the pre-heating stage, when the reactor temperature reaches 340 K, the reaction is assumed to start and it corresponds to the initial reaction time $t = 0$ which is thus difficult to determine exactly. Later, the reactor temperature will take a value between 348 and 355 K, as it will be explained in next section.

2.4. Minimization of batch time with T as control variable

In the first case, in order to maximize the productivity of the industrial polymerization reactor, i.e. to minimize the final batch time, the optimal temperature profile is calculated. Temperature is chosen because of its large influence on the polymerization reaction and polymer properties. The opti-

mization problem can be formulated as

$$
\begin{array}{ll}
\min_{T(t)} & \displaystyle\int_{t_0}^{t_f} dt = t_f - t_0 \\
s.t. & \dot{x}_i = f_i(x(t), T(t), t)\ ,\ i = 1, ..., 7 \text{ and } \forall t \in [t_0, t_f]\ , \quad \text{state model} \\
& x_1(t_0) = 5\ , \quad \text{initiator moles} \\
& x_2(t_0) = 4000\ , \quad \text{total monomer moles} \\
& x_3(t_0) = 4000\ , \quad \text{residual monomer moles} \\
& x_i(t_0) = 0, \quad i = 4, ..., 7\ , \quad \text{initial conditions} \\
& x_f \geq 0.95\ , \quad \text{final conversion} \\
& \bar{M}_{n_f} \geq 1.8 \times 10^5\ , \quad \text{final number average molecular weight} \\
& \phi_S \geq 46\%\ , \quad \text{final solids content} \\
& 348\text{K} \leq T(t) \leq 355\text{K}\ , \quad \text{temperature interval}
\end{array}
\tag{12}
$$

Table 3: Dynamic optimization case using T as control variable: Influence of the number of time increments on the optimization results

N_u	t_f (s)	x_f	$M_{n,f} \times 10^{-5}$	$M_{w,f} \times 10^{-5}$	D
3	26463	0.9625	2.6217	5.7279	2.18
5	26458	0.9655	2.6341	5.7907	2.19
10	26347	0.9678	2.6161	5.7509	2.19
20	26214	0,9706	2.6586	5.8062	2.18

The monomer and initiator flow rates are constant according to the recipe of Table 2. The value of monomer flow rate corresponds approximately to the ratio of the monomer quantity of the industrial recipe over the duration of the fed-batch time, similarly for the initiator flow rate. Indeed, as the final time is not known before dynamic optimization, the monomer is fed from $t = 70$ min with a flow rate of 2.1 mol/s, whereas the maximum authorized flow rate in the industrial operation is 2.3 mol/s. The initiator flow rate is 1×10^{-3} mol/s also from $t = 70$ min (Figures 9a and 9b). Then, the operation is performed in two stages, the first one in batch mode (without addition of reactants) and the rest of the operation in fed-batch mode where monomer and initiator are fed to the reactor. Consequently, two different models are used, one for the batch operation, followed by another one for the fed-batch. Dynamic optimization is applied to the entire operation, i.e. including the batch mode and fed-batch mode stages (Figure 8).

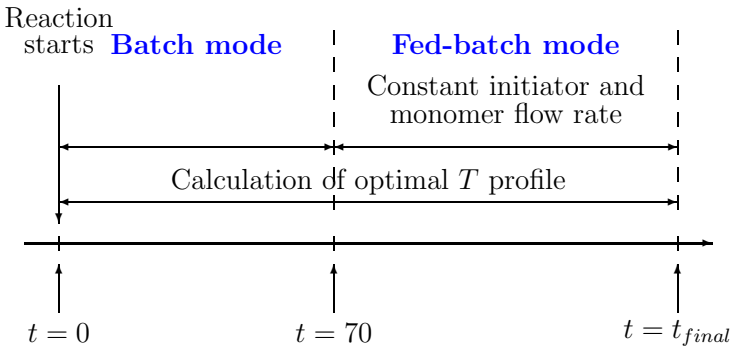

Figure 8: Dynamic optimization case using T as control variable: Scheduling of operations

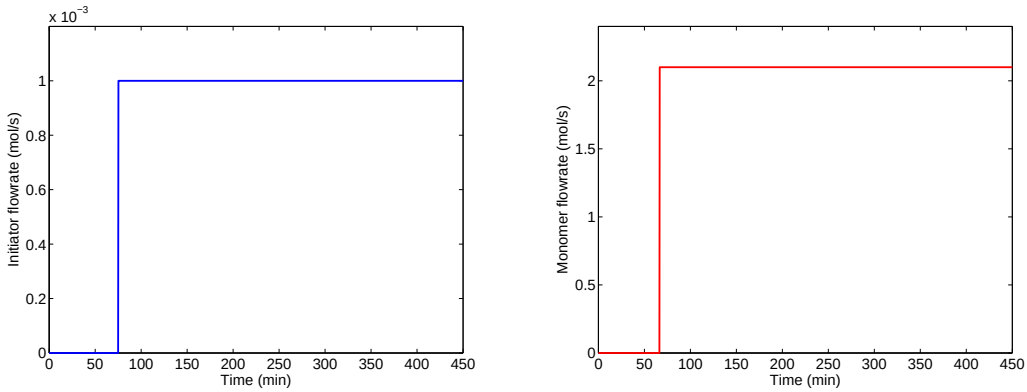

(a) (b)

Figure 9: Dynamic optimization case using T as control variable: Feed policies, Initiator flow rate (a), Monomer flow rate (b)

The influence of the number N_u of discrete time segments used during the total reaction time has been studied. Thus, four different discretization scenarios were calculated considering N_u equal to 3, 5, 10 and 20, the temperature taken as the control variable being piecewise constant on each time interval. Table 3 shows the influence of the number of discrete time increments on the most important quality indicators of the final polymer. As it can be observed, the total batch time decreases little with the increase of the number of piecewise controls. At the same time, the overall quality of the polymer such as the conversion and the average molecular weight is very little influenced by the increase of the number of time increments.

Figures 10 and 11 show the influence of the number of time increments

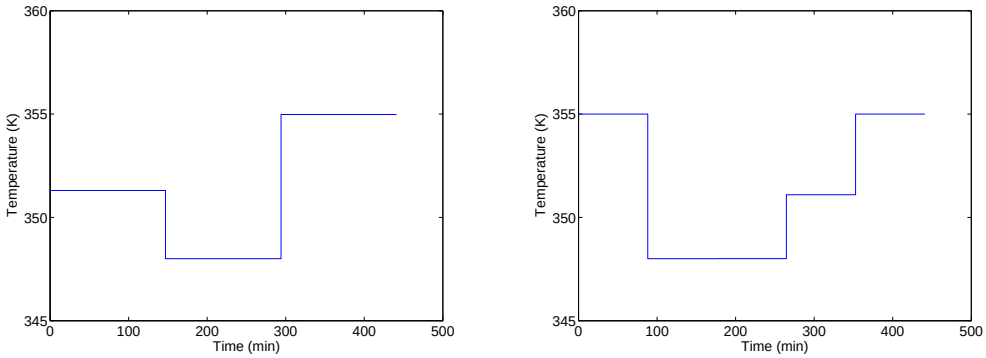

(a) $N_u = 3$ (b) $N_u = 5$

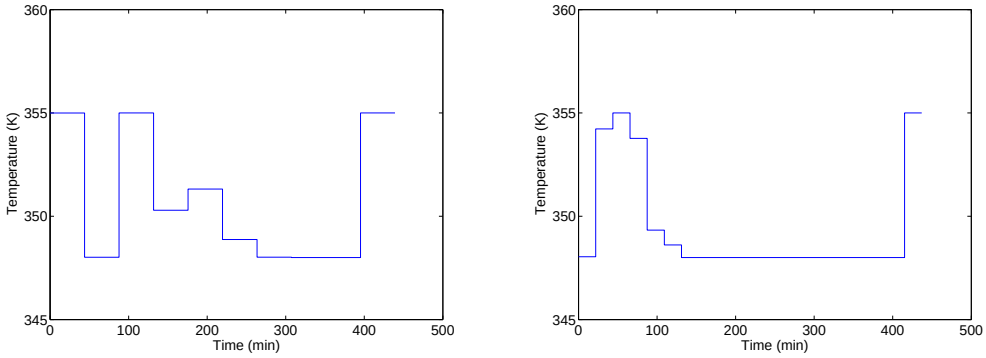

(c) $N_u = 10$ (d) $N_u = 20$

Figure 10: Dynamic optimization case using T as control variable: Influence of the number of time increments on the optimal temperature profile

respectively on the optimal temperature profiles and on the corresponding quality results for values of N_u of 5, 10 and 20. In spite of important variations of the temperature profile, it has little influence on the final characteristics of polymerization. In all the optimization runs, at the end of the process, the temperature increases to reduce the variation of the molecular weight M_n and reach the final value close to the corresponding constraint. The chain length decreases when temperature increases due to the transfer reactions, which induces the entry of radicals to the particles. This results finally in instantaneous termination reaction of these radicals inside the particles. It must be noted that the same strategy of temperature increase, at the end of the operation, is currently used by the operators of the reactor at the company. In the same way, Figures 11a, 11c and 11e show that the

rate of change of conversion in time is directly proportional to the temperature. Figures 10a and 10c show that the temperature often switches from the lower bound to the upper bound and viceversa, in particular at the start and close to the end of the total reaction time. This behaviour is typical from minimum time problems and is known as *bang- bang* control (Corriou, 2004, 2012; Chachuat, 2007). Many systems in chemical engineering and in other domains are controlled in on-off mode, in a way similar to *bang-bang* control.

2.5. Minimization of batch time with reactor T and q_I as control variables

In the second optimization problem, one additional optimization variable is considered. Here, the initiator flow rate is also used as a control variable due to its large effect on the monomer conversion and molecular properties of the final product. Again, the objective is to minimize the final reaction time, and in consequence the optimal temperature and initiator flow rate profiles are calculated. In this case, the optimization problem is formulated as

$$
\begin{array}{ll}
\min_{T(t),q_I(t)} & \displaystyle\int_{t_0}^{t_f} dt = t_f - t_0 \\
s.t. & \dot{x}_i = f_i(x(t), T(t), q_I(t), t) \ , \quad i = 1, ..., 7 \\
 & \text{and} \quad \forall t \in [t_0, t_f] \quad \text{state model} \\
 & x_1(t_0) = 5 \ , \quad \text{initiator moles} \\
 & x_2(t_0) = 4000 \ , \quad \text{total monomer moles} \\
 & x_3(t_0) = 4000 \ , \quad \text{residual monomer moles} \\
 & x_i(t_0) = 0 \ , \quad i = 4, ..., 7 \quad \text{initial conditions} \\
 & x_f \geq 0.99 \ , \quad \text{final conversion} \\
 & \bar{M}_{n_f} \geq 2.1 \times 10^5 \ , \quad \text{final number average molecular weight} \\
 & \phi_S \geq 49\% \ , \quad \text{final solids content} \\
 & 348K \leq T(t) \leq 355K \ , \quad \text{temperature interval} \\
 & q_I(t) \leq 0.8 \times 10^{-3} \text{mol/s} \ , \quad \text{initiator flow rate interval}
\end{array}
\tag{13}
$$

The constant monomer flow rate injected during the fed-batch stage starting at t =70 min takes the same value as in section 2.4. Initiator flow rate and temperature are used as control variables according to the optimization problem formulated in equation (13). In the first part of the reaction, the process is operated in batch mode, with respect to the monomer input. A scheme of the operation is shown in Figure 12. As in the first problem, a

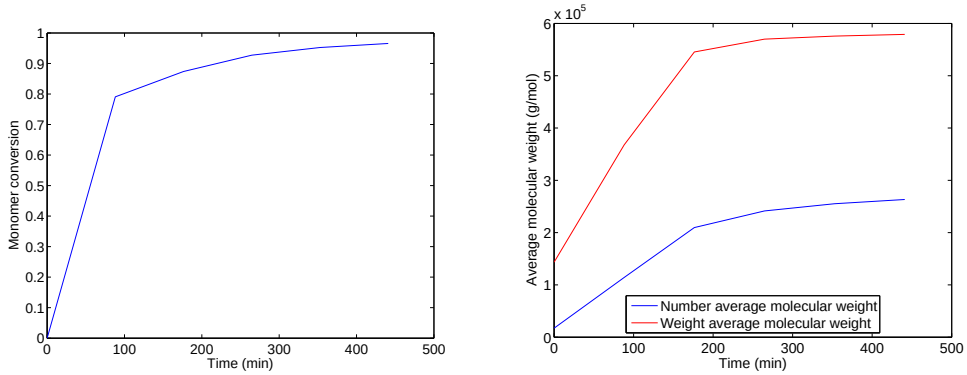

(a) $N_u = 5$

(b) $N_u = 5$

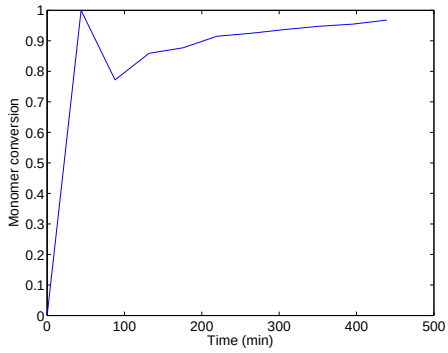

(c) $N_u = 10$

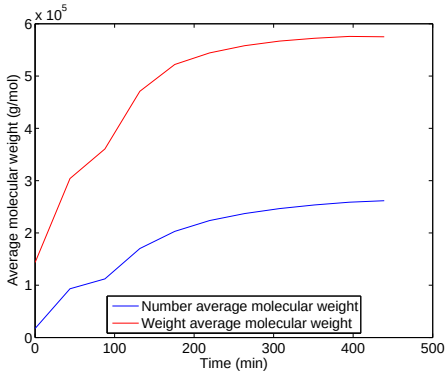

(d) $N_u = 10$

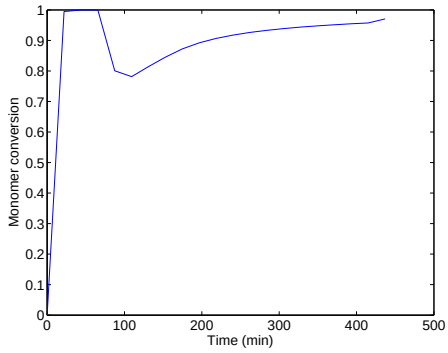

(e) $N_u = 20$

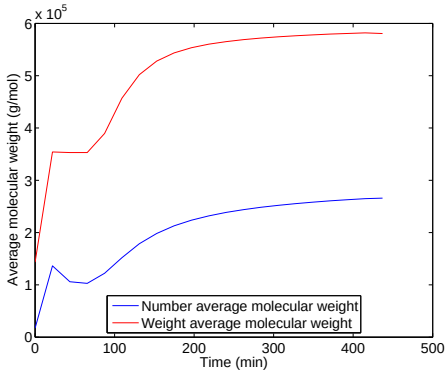

(f) $N_u = 20$

Figure 11: Dynamic optimization case using T as control variable: Quality results. Left column: monomer conversion. Right column: average molecular weight.

piecewise discretization using 3, 5, 10 and 20 control segments was studied.

Table 4: Dynamic optimization case using T and q_I as control variables: Optimization results

N_u	t_f (s)	x_f	$M_{n,f} \times 10^{-5}$	$M_{w,f} \times 10^{-5}$	D
3	29510	0.9900	2.1654	4.9164	2.27
5	29527	0.9901	2.2398	5.1804	2.31
10	28872	0.9900	2.1155	4.8532	2.29
20	27118	0,9900	2.2825	5.2814	2.31

Table 4 shows the results for the four optimization runs. For this second dynamic optimization problem, the constraint of the minimum conversion was increased from 95% to 99%. For this reason, the final times are slightly larger than those obtained previously. However, the conversion has been increased importantly which is beneficial for the process efficiency. The reaction times calculated here are approximately 9% lower than the typical reaction time in the plant, thus improving the productivity of the process.

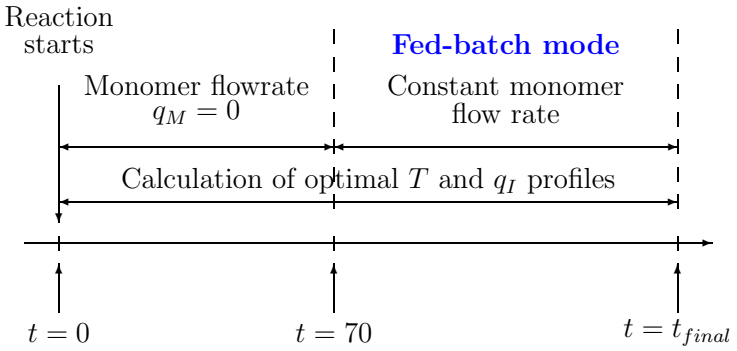

Figure 12: Dynamic optimization case using T and q_I as control variables: Scheduling of operations

Again, it can be noted that the total reaction time decreases with the increase of N_u, but the final values of the average molecular weight and the dispersity of the polymer do not vary significantly.

Figures 13 and 14 show the optimal temperature profile and optimal initiator flow rate profile, respectively. Again, the *bang-bang* control tendency is observed for the temperature and a similar behaviour is observed for the initiator when $N_u = 20$ (Figure 14d). Also, the multivariable nature of the system is observed. The initiator flow rate and the reaction temperature appear to be correlated. In the first half of the operation, the tendency is

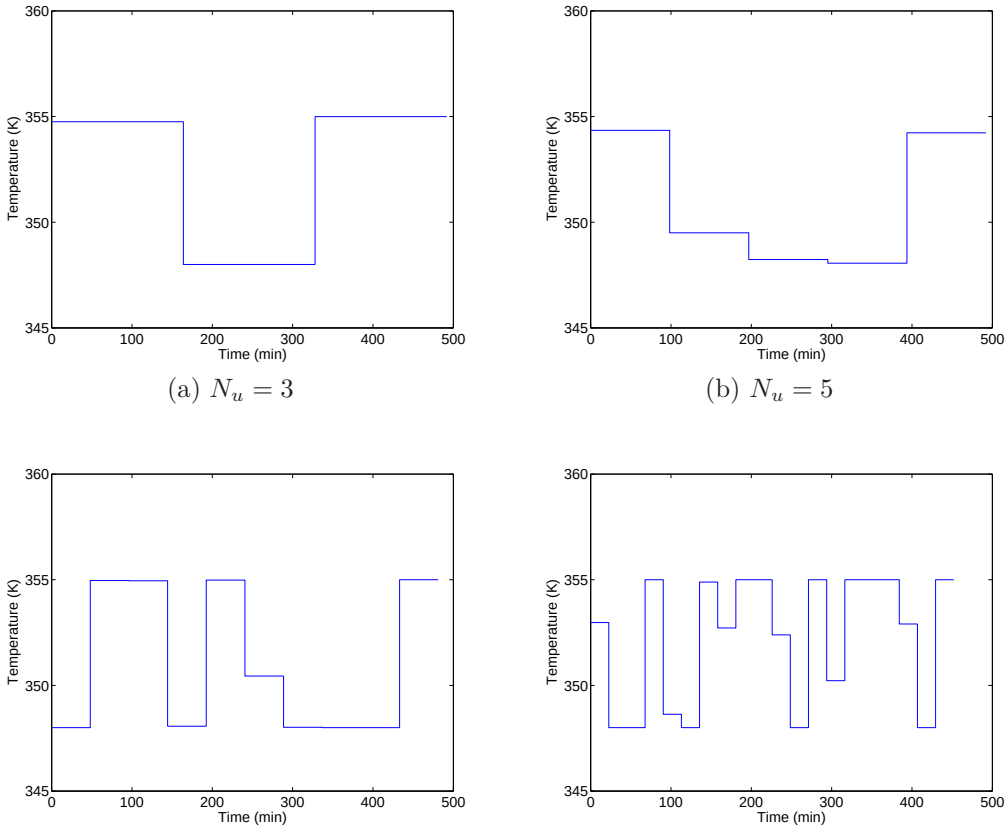

(a) $N_u = 3$ (b) $N_u = 5$

(c) $N_u = 10$ (d) $N_u = 20$

Figure 13: Dynamic optimization case using T and q_I as control variables: Optimal temperature profile

marked by low values of initiator flow rate and intermediate values of the temperature. In the second half, additional injections of initiator are calculated and often compensated by temperature decreases. However, it is difficult to observe only one specific response, taking into account that different discretization scenarios exist and interactions occur at the same time. When the initiator flow rate is increased, the chain growth rate decreases because more monomer can react with the additional initiator to promote more initiation reactions instead of propagation of the polymer chain. Finally, in order to control the last part of the reaction, temperature and initiator flow rate increase so that the final average molecular weight and conversion satisfy the final constraints. The increases of temperature and initiator in the

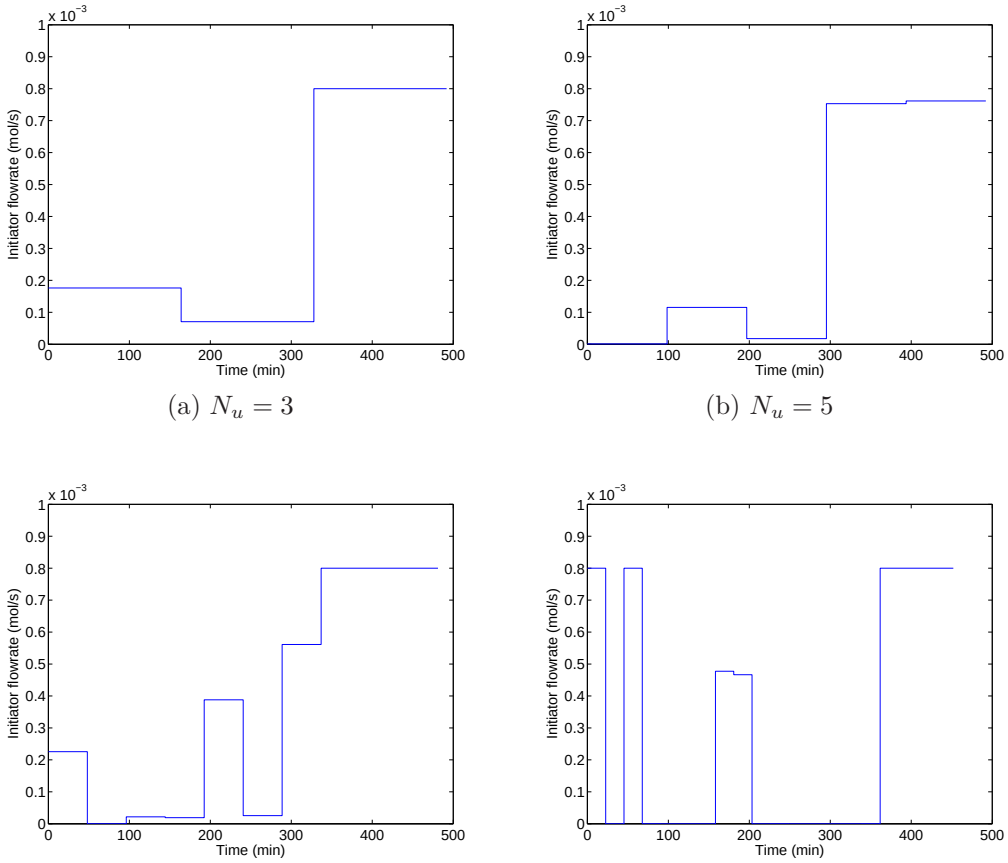

(a) $N_u = 3$ (b) $N_u = 5$

(c) $N_u = 10$ (d) $N_u = 20$

Figure 14: Dynamic optimization case using T and q_I as control variables: Optimal initiator flow rate profile

reactor increase the polymerization rate and the conversion, and reduce the final molecular weight (Figure 15).

2.6. Minimization of batch time with T, q_I and q_M as control variables

The third optimization problem involves three control variables: temperature, initiator flow rate and monomer flow rate. These three variables are easily controlled in the industrial reactor and therefore are susceptible to be changed at the same time to achieve a desired performance of the reactor. Taking into account that vinyl acetate has a high rate of radical transfer to polymer, the monomer feed flow rate has an important effect on the molecular weight. For that reason, it is also considered in this optimization case

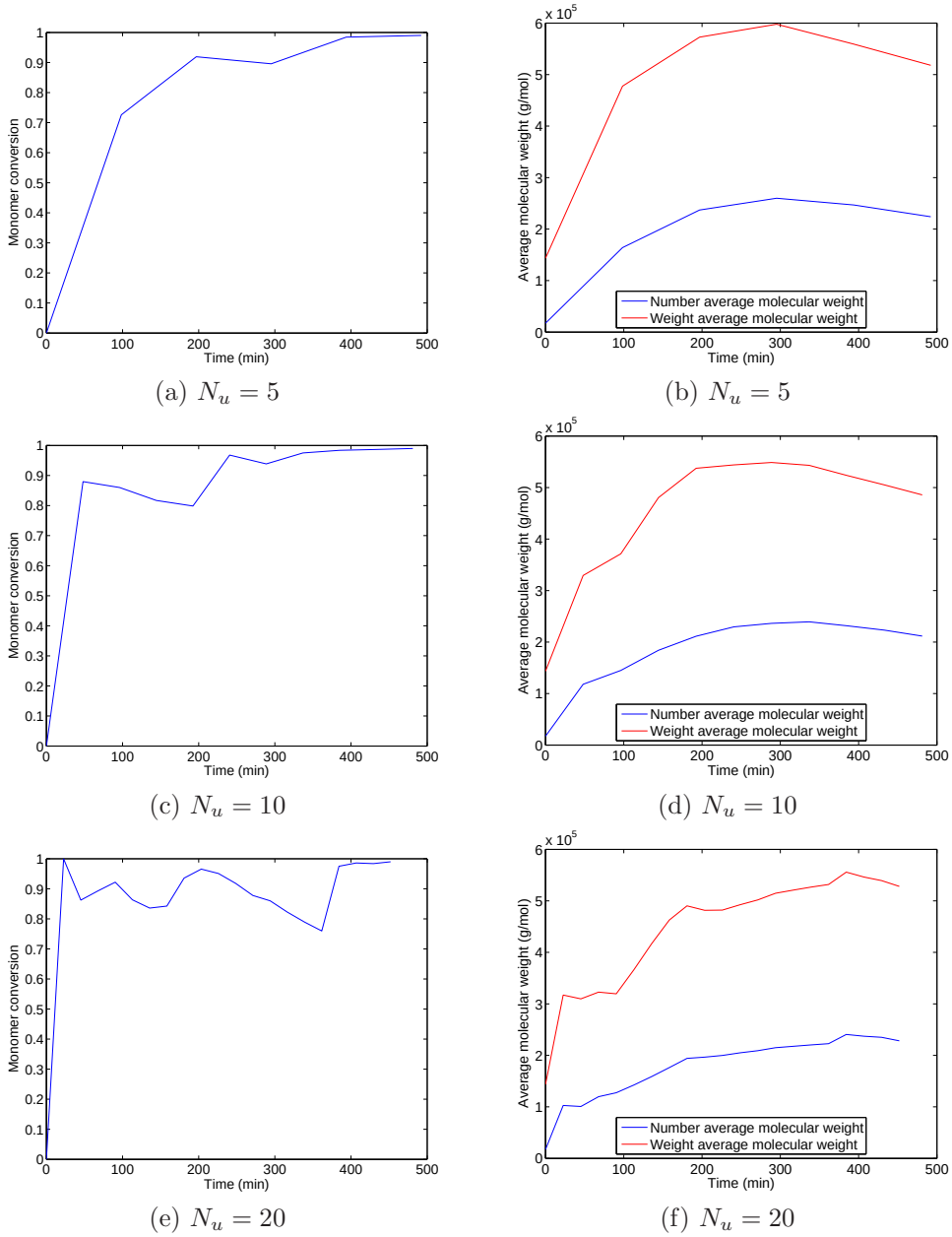

(a) $N_u = 5$ (b) $N_u = 5$

(c) $N_u = 10$ (d) $N_u = 10$

(e) $N_u = 20$ (f) $N_u = 20$

Figure 15: Dynamic optimization case using T and q_I as control variables: Quality results. Left column: monomer conversion. Right column: average molecular weight.

as a control variable. The optimization problem is formulated as

$$
\begin{array}{ll}
\min_{T(t),q_I(t),q_M(t)} & \int_{t_0}^{t_f} dt = t_f - t_0 \\
s.t. & \dot{x}_i = f_i(x(t), T(t), q_I(t), q_M(t), t) \quad i = 1, ..., 7 \\
& \text{and} \quad \forall t \in [t_0, t_f] \quad \text{st. model} \\
& x_1(t_0) = 5 \ , \quad \text{initiator moles} \\
& x_2(t_0) = 4000 \ , \quad \text{total monomer moles} \\
& x_3(t_0) = 4000 \ , \quad \text{residual monomer moles} \\
& x_i(t_0) = 0 \ , \quad i = 4, ..., 7 \quad \text{initial conditions} \\
& x_f \geq 0.992 \ , \quad \text{final conversion} \\
& \bar{M}_{n_f} \geq 2.2 \times 10^5 \ , \quad \text{final number average molecular weight} \\
& \phi_S \geq 50\% \ , \quad \text{final solids content} \\
& 348K \leq T(t) \leq 355K \ , \quad \text{temperature interval} \\
& q_I(t) \leq 0.8 \times 10^{-3} \text{mol/s} \ , \quad \text{initiator flow rate interval}
\end{array}
$$

The monomer flow rate, initiator flow rate and temperature profiles were determined according to the dynamic optimization problem formulated in equation (14). In this case, fed-batch operation mode is used as the unique operation mode for the dynamic optimization calculations (Figure 16). As in the two last cases, a piecewise discretization using 3, 5, 10 and 20 control segments was studied. Table 5 shows the results for the four optimization runs. The final conversion constraint here is slightly higher than the conversion constraint used in the dynamic optimization based on temperature and initiator flow rate as control variables. This is mentioned because the final time obtained here is lower than the minimum time calculated in the two previous cases where the conversion constraint was lower as well as the constraints of molecular weight and solids content. The most interesting result of this optimization case is the final time obtained when using 10 and 20 piecewise controls.

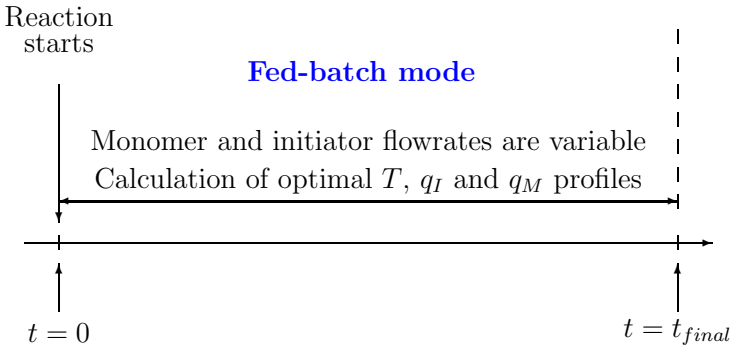

Figure 16: Dynamic optimization case using T, q_I and q_M as control variables: Scheduling of operations

In this case, the influence of the number of time intervals or piecewise controls used is more evident because more degrees of freedom exist that promote interactions during the reaction. This multivariable problem with three control variables allows the optimization solver to more easily find optimal operating values of the process variables which minimize the total reaction time. Specifically, in the case of 20 piecewise controls, a total time of 23762 seconds is obtained (Figure 17). This optimal final time is at least 20% lower than the current batch time used in the plant to perform this polymerization.

Optimal profiles are shown in Figures 17, 18 and 19 for temperature, initiator flow rate and monomer flow rate, respectively. The influence of

Table 5: Dynamic optimization case using T, q_I and q_M as control variables: Optimization results

N_u	t_f (s)	x_f	$M_{n,f} \times 10^{-5}$	$M_{w,f} \times 10^{-5}$	D
3	29338	0.9920	2.4041	5.6376	2.34
5	28426	0.9920	2.6186	6.0685	2.32
10	26678	0.9920	2.1999	5.1265	2.33
20	23762	0.9920	2.2000	5.1171	2.32

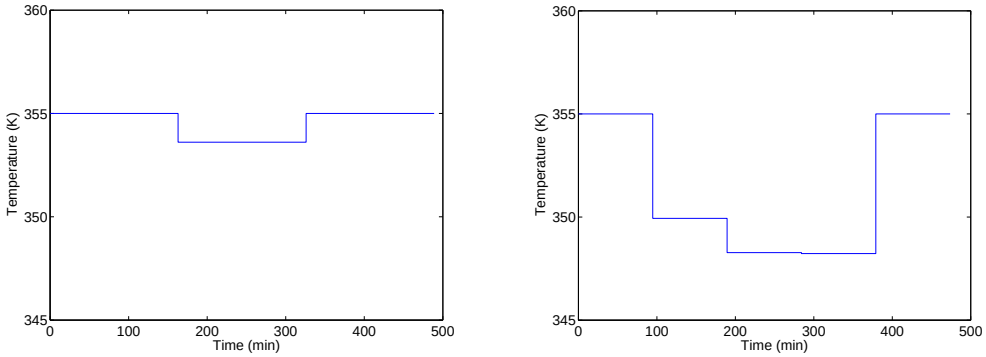

(a) $N_u = 3$ (b) $N_u = 5$

(c) $N_u = 10$ (d) $N_u = 20$

Figure 17: Dynamic optimization case using T, q_I and q_M as control variables: Optimal temperature profile

increasing the initiator flow rate on the polymerization rate can be noticed in Figures 18b, 18c and 18d, and Figures 20a, 20c and 20e. In these two cases, the initiator flow rate is augmented at a reaction time of 200 min, and

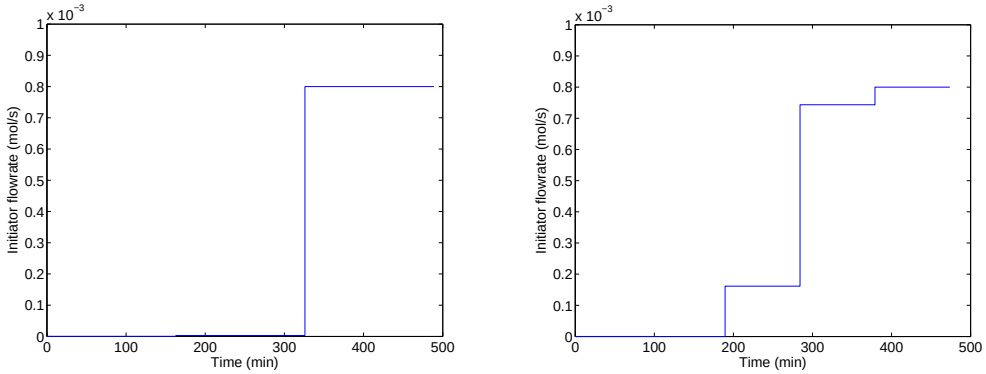

(a) $N_u = 3$ (b) $N_u = 5$

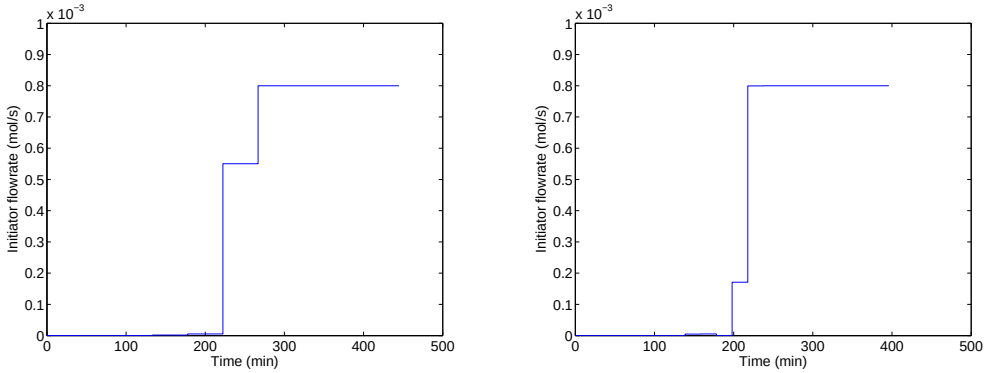

(c) $N_u = 10$ (d) $N_u = 20$

Figure 18: Dynamic optimization case using T, q_I and q_M as control variables: Optimal initiator flow rate profile

immediatly the conversion increases. The initiator flow rate is maintained at low values (close to zero) during the first part of the operation in which monomer is being fed, and only in the last part of the operation, the initiator flow rate is increased in order to accelerate the polymerization and reduce the final content of monomer (Figure 18). At the same time, the monomer flow rate is maintained at high values, close or equal to the upper bound, during the major part of the reaction, and finally is decreased when the polymerization is ending (Figure 19). In the real plant operation, the initiator is fed almost continuously and this differs largely from the optimal policy obtained by dynamic optimization where some initiator is fed at the end of the reaction. Also, in the real plant, reactor temperature is maintained

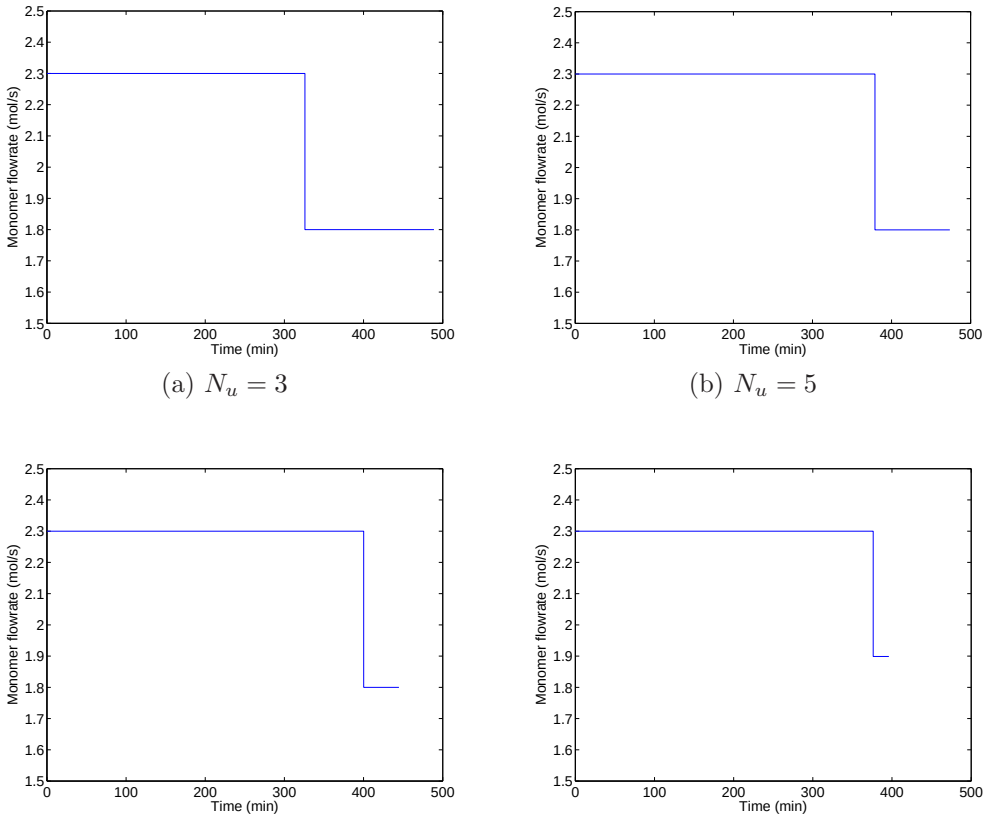

(a) $N_u = 3$ (b) $N_u = 5$

(c) $N_u = 10$ (d) $N_u = 20$

Figure 19: Dynamic optimization case using T, q_I and q_M as control variables: Optimal monomer flow rate profile

approximately constant by manual operation during the reaction without using the jacket, but only by means of the sensible heat of the monomer and initiator fed to the reactor. In the present study, the proposition will be to use the jacket for heat exchange, but to feed the reactor in monomer and initiator according to the optimal policy and control the temperature by means of a nonlinear controller. In the same way as the initiator takes a maximum value just before the final time, it can also be noticed that the temperature increases to its upper bound during the final control segment also trying to reduce the residual monomer of the polymer (Figure 17).

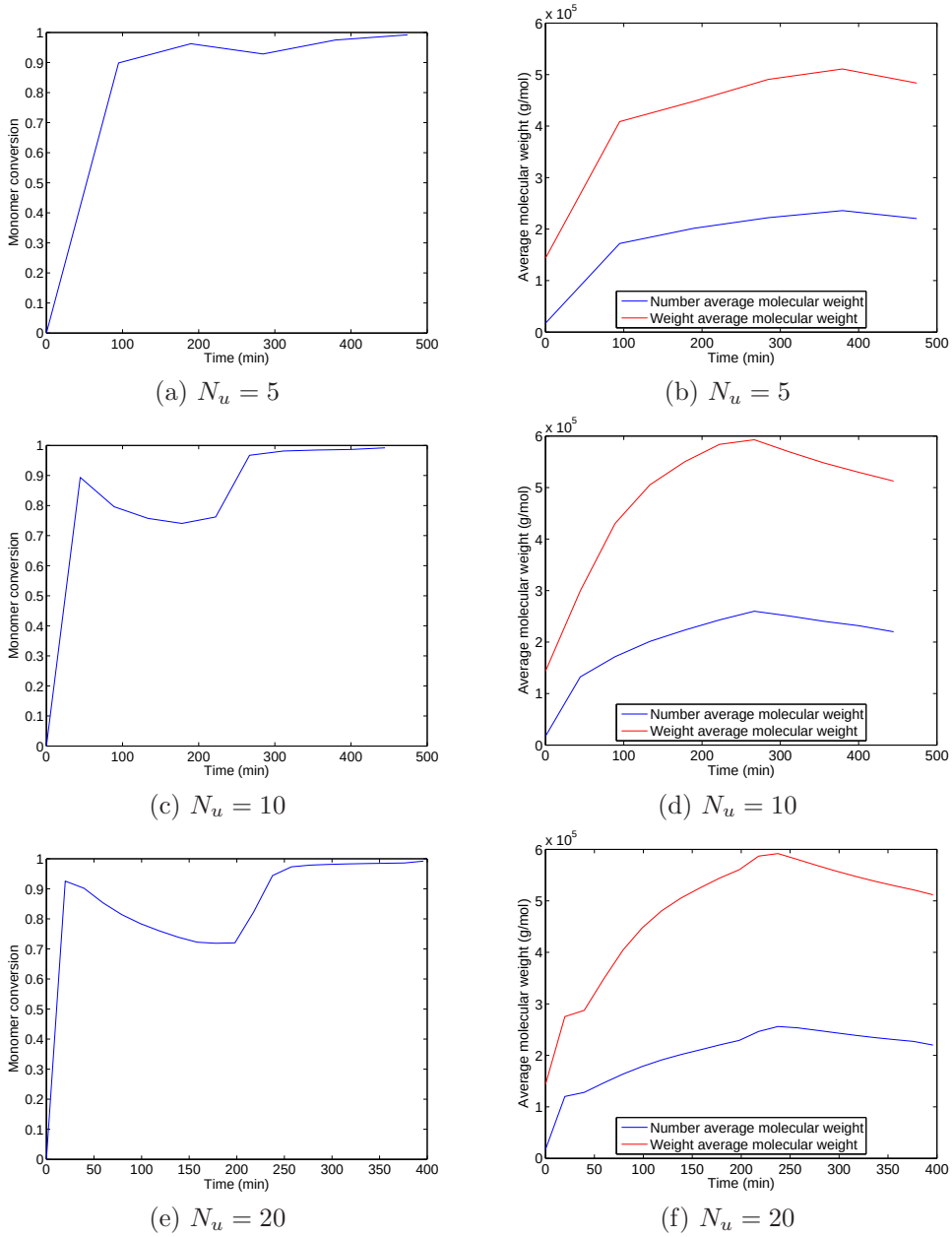

(a) $N_u = 5$ (b) $N_u = 5$

(c) $N_u = 10$ (d) $N_u = 10$

(e) $N_u = 20$ (f) $N_u = 20$

Figure 20: Dynamic optimization case using T, q_I and q_M as control variables: Quality results. Left column: monomer conversion. Right column: average molecular weight

3. Nonlinear geometric control and state estimation

In this section, a nonlinear geometric temperature controller is applied to the industrial emulsion polymerization reactor. Temperature is controlled by

a nonlinear controller designed in our previous work (Gil et al., 2014). The optimal temperature profile calculated in the last section is used here as the set point of the temperature control loop. The optimal feed policies of initiator and monomer are also used here as set points supposing an automatic regulatory control for these two flow rates. Figure 21 shows a schematic representation of the control loops and the use of dynamic optimization results. Conversion and polymer quality results obtained are compared with those corresponding to the current operation data.

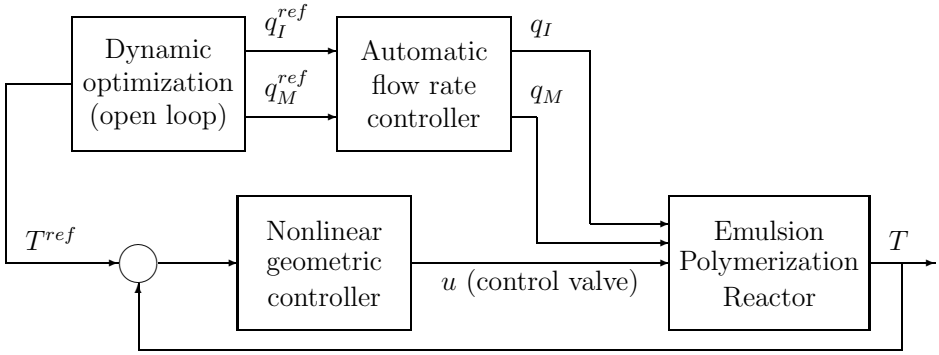

Figure 21: Schematic representation of the control of the emulsion polymerization reactor

The controlled output is the temperature of the reactor contents T. The position u of a three-way valve is used as a manipulated input that imposes the respective flow rates through the cold and hot heat exchangers so that the inlet coolant temperature $T_{j_{in}}$ could also be considered as the manipulated variable. Thus, the controlled system is reduced to Single Input Single Output.

Two models are used, on one side a complete detailed model considered as the plant describing the dynamic reactor behavior and the polymerization reaction, including the moments of the polymer chains described in eqs (5-7). On the other side, in order to simplify the nonlinear geometric control law and the state estimation, a reduced model is built with the following reduced state vector for control and estimation

$$\boldsymbol{x} = (I, M_t, M_M, V_{pol}, T, T_j) \tag{15}$$

where the three moments of the polymer chains are not taken into account (Gil et al., 2014). Among these states, I, M_t and V_{pol} are not observable and they are only predicted, i.e. they are obtained by simple integration of the

differential equations without correction. The continuous-discrete extended Kalman filter is implemented to estimate the three states M_M, T, T_j which are used in the nonlinear control law. The controller and the observer share the same input and output. It must be noted that the state estimations or predictions which are provided are useful also for monitoring of the reactor. The details of the extended Kalman filter as well as the nonlinear control law are presented in Gil et al. (2014).

3.1. Control under optimal conditions

Now, it is important to show that a nonlinear geometric controller is capable of tracking the optimal temperature trajectories with the combined use of the optimal feed policies calculated for the initiator and the monomer. It must be noted that the dynamic optimization was performed in open loop using only the kinetic model without the energy balances of the reactor. The nonlinear controller of course makes use of the same kinetic model but with the energy balances. Thus, apart from the study of temperature tracking, it will be interesting to compare the various characteristics of the polymer obtained in open loop and in closed loop, such as viscosity, conversion, number average molecular weight.

3.2. Optimal temperature control with optimal feed policies (q_I and q_M)

The most interesting result of the dynamic optimization study is the minimization of the reaction time (maximization of productivity). Now, it will be supposed that the reactor is operated under the operating conditions found in section 2.6 and following the recipe defined for the industrial operating conditions in Table 2. The case of the dynamic optimization using also the three control variables and N_u equal to 20 is discussed here. The nonlinear geometric controller presents a good performance for tracking the temperature trajectory calculated by means of dynamic optimization (Figure 22a). At the end of the operation, the temperature increases up to the upper limit (355 K) and also the initiator flow rate is increased in order to end the reaction and satisfy the final constraints (Figure 22a).

The controller works well to remove the reaction heat (Figure 22e) and maintain the temperature close to the optimal set point previously established (Figure 22a). After preheating stage (the first 80 min) where the seed is formed, the monomer conversion increases up to 99.2% as in the dynamic optimization problem. It is interesting to note that, according to the dynamic optimization results, the temperature is maintained at the minimum

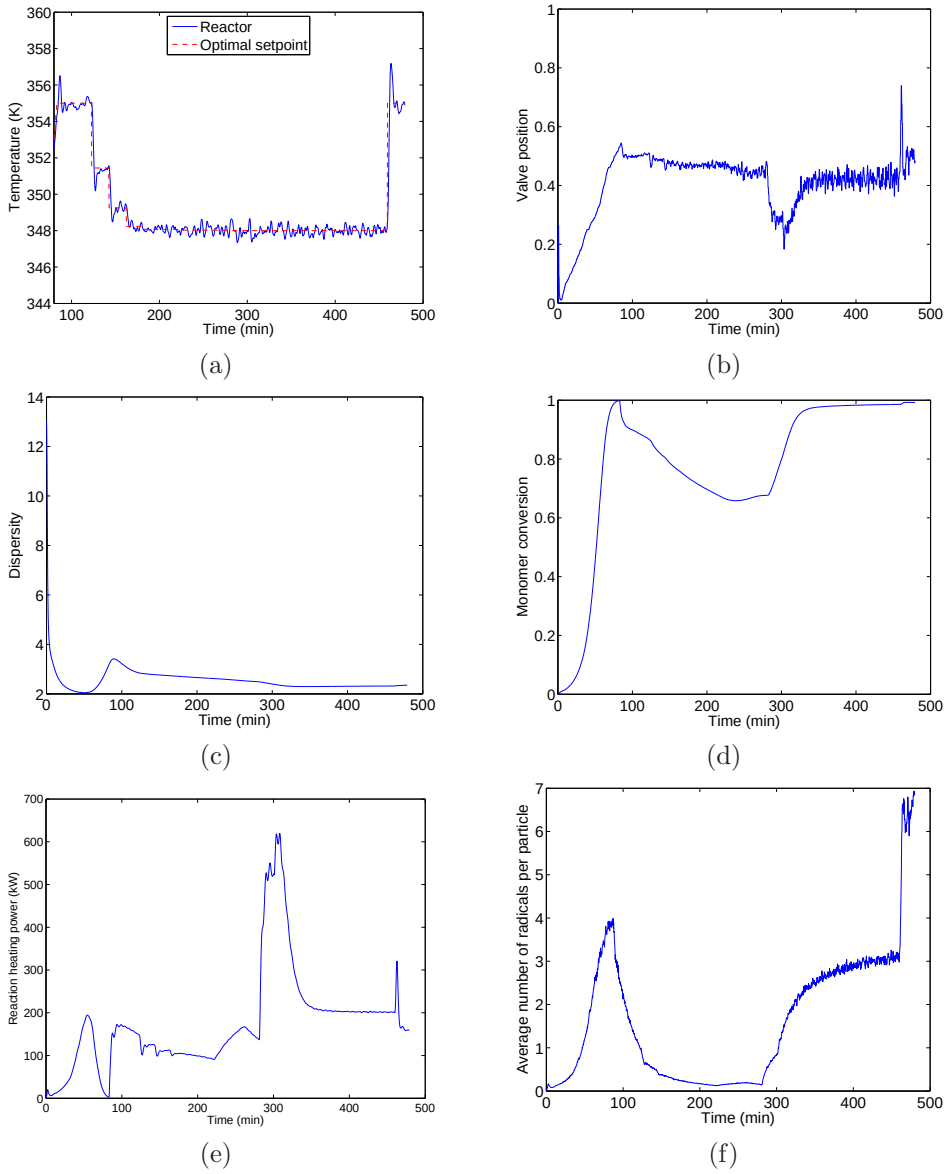

Figure 22: Nonlinear geometric control of the emulsion polymerization reactor with time minimization using q_I, q_M and T as optimization variables and $N_u = 20$. a) Optimal temperature profile b) Valve position; c) Dispersity d) Monomer conversion; e) Reaction power f) Average number of radicals per particle

409 constraint during a large part of the operation. Only in the last part, the
410 temperature is increased rapidly in order to end the reaction. The initia-

tor flow rate also increases at the end of the reaction to satisfy the final constraints related with the final molecular weight. This demands an additional effort from the controller which is compensated, in principle, by the control valve (Figure 22b) but also it compensates the release of an important additional quantity of heat (Figure 22e). However, it is clear that the controller is capable of following the temperature setpoint. Consequently, the desired conversion and quality results are obtained. Another interesting observation from Figure 22f is that the average number of radicals per particle $\bar{n}$ increases importantly at the end of the operation, due to the final large injection of initiator calculated by the optimization. The low radical desorption rate with respect to radical entry rate produces a large increase of the heat released by the reaction and, simultaneously, the viscosity at the end of the operation increases up to 1200 P, limiting the mobility of radicals and favoring the increase of the temperature. All these observations could indicate a gel effect phenomenon which also accompanies final conversions as high as 99.2%. However, again, this is satisfactorily managed by the controller as it can be observed in the last 20 minutes in Figure 22a. Table 6 summarizes the constraints established in two of the dynamic optimization cases studied and the results obtained with the application of the nonlinear control to these optimal scenarios. It can be noted that, in all the cases, the constraints previously defined in dynamic optimization calculations are also satisfied when applying the nonlinear control to the simulated plant.

Table 6: Results for the constraints established in the dynamic optimization. CDO: Constraint in Dynamic Optimization, CS: Control simulation

	Number average molecular weight		Final conversion		Solids content (%)	
N_u	CDO	CS	CDO	CS	CDO	CS
5	2.2×10^5	2.259×10^5	0.992	0.9921	50	53.1
20	2.2×10^5	2.269×10^5	0.992	0.992	50	50

3.3. Robustness tests

The robustness of the nonlinear controller coupled with state estimation is studied with respect to typical modeling errors or real situations found in the normal plant operation. For that purpose, the rigorous model of the plant, representing the process, remains the same as it was defined in section 2.1 while the simplified model used in control calculations is modified by introducing modeling errors. Four different scenarios were supposed: errors

about the propagation reaction constant, heat of reaction and heat transfer coefficient values, and a change in the temperature of the coolant used in the reactor cooling. In the first robustness test, it was assumed that the propagation constant is reduced by 50% with respect to its real value. Thus, the reaction rate calculated in the reduced model of the state estimator is lower than the real rate of the process, and therefore also the estimation of the reaction heat produced. The second test consisted in increasing by 50% the value of the heat of the reaction reducing the exothermicity of the reaction. In the third robustness test, it was assumed that the heat transfer coefficient U is decreased by 40% with respect to its real value. This is representative of changes due to equipment fouling and variations in the viscosity and the solids content of the reacting mixture that also affect the value of U. Finally, in the last test, the coolant temperature was increased from 293 to 300 K simulating a failure in the cooling tower of the plant. Thus, the value of the inlet jacket temperature considered in the reduced model is erroneous and this influences the energy balances.

The main effect of these robustness tests is observed about the estimated monomer conversion (Figure 23). In the first 300 minutes, the difference between the estimated monomer conversion and the real value is slight for the cases where errors about heat transfer coefficient (Figure 23a) and heat of reaction (Figure 23b) were introduced. In spite of important differences with respect to the real values, the controller works well and the monomer conversion is well estimated. On the other way, the errors due to the change in the coolant temperature and propagation rate constant are more important with differences around 10% at maximum compared with the actual monomer conversion. Globally, the same tendency is maintained up to 300 minutes, but, in the last part of the operation (between 300 and 500 minutes), the deviation between the estimated and calculated values is large in three of the four cases. This deviation is caused by the addition of an important quantity of initiator at time $t = 300$ min. The initiator accelerates the reaction, an additional quantity of heat is released and the average number of particles also increases promoving a gel effect in the system. Also, it should be mentioned that, in the last part of the operation, the solids content and viscosity increase importantly modifying heat and mass transfer coefficients. However, a good temperature control is achieved in all cases (Figure 24) demonstrating the efficiency of nonlinear control and its robustness.

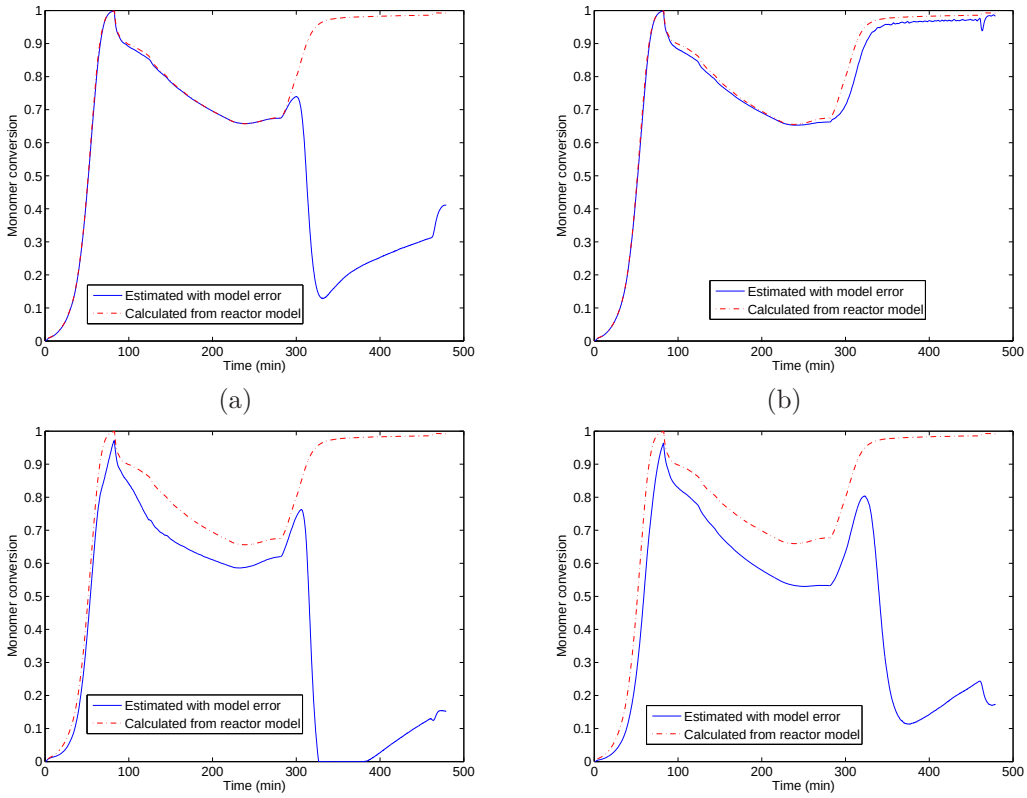

Figure 23: Influence of the robustness tests on the monomer conversion. a) Heat transfer coefficient error; b) Reaction heat error; c) Coolant temperature error; d) Propagation constant error

4. Conclusion

The dynamic optimization of the emulsion polymerization of vinyl acetate was studied. Three different optimization scenarios were established from the more simplistic (only one control variable) to the more complex (three control variables) in order to minimize the reaction time. Constraints are imposed with respect to some polymer desired qualities (conversion, molecular weight and solids content) as well as allowed flow rates and reactor temperature. Piecewise constant profiles were assumed and the influence of time discretization was studied. The influences of initiator, temperature and monomer were identified. In all the cases, the control variables often change during the batch according to the well-known *bang-bang* effect, typical of

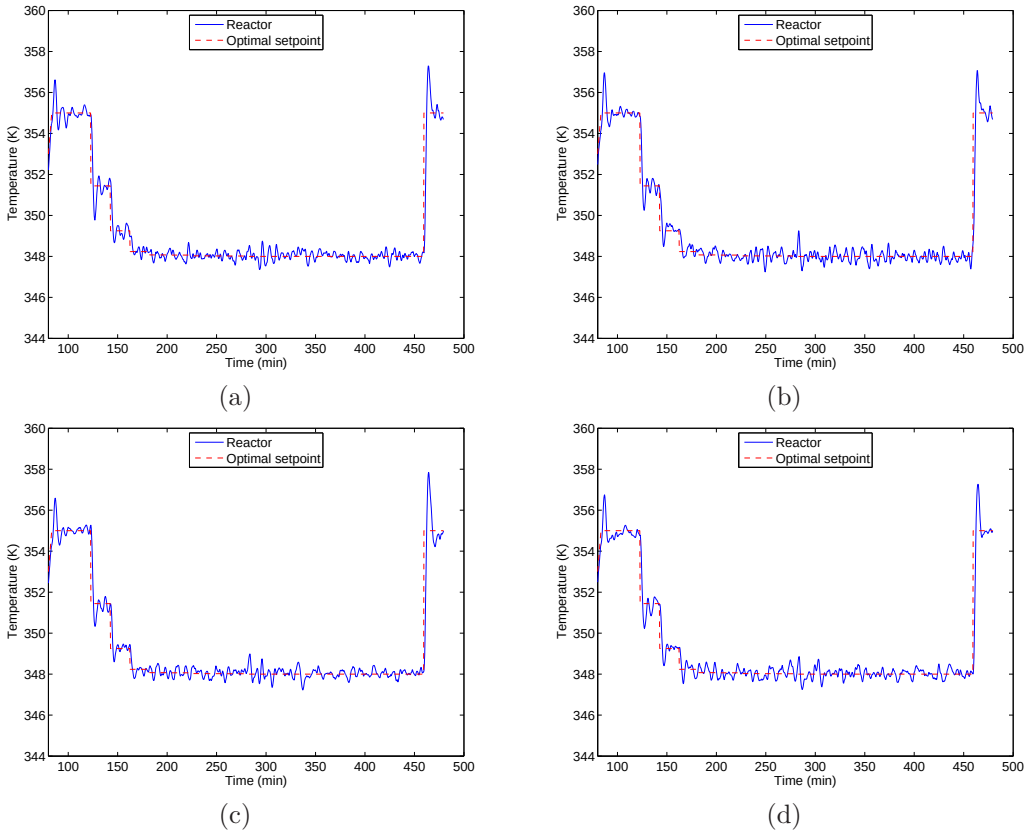

Figure 24: Influence of the robustness tests on the reactor temperature control. a) Heat transfer coefficient error; b) Reaction heat error; c) Coolant temperature error; d) Propagation constant error

minimum time dynamic optimization problems. It can be noticed that the most efficient results are obtained when three variables, i.e. T, q_I and q_M are simultaneously used as control variables. A reduction of 20% of the batch time was achieved with respect to the normal operating conditions applied at the chemical company.

A nonlinear controller was used to track the temperature in the polymerization reactor in spite of typical disturbances such as initiator and monomer injections. The optimal temperature profile, obtained by a dynamic optimization study, was used as the set point for the nonlinear control. In the same time, the optimal feed policies of monomer and initiator were followed by means of a regulatory control of their flow rates. The results show that

the nonlinear controller is appropriate to track the optimal temperature trajectories calculated previously. Also, the final temperature increase due to the initiator injection is rapidly corrected by the controller action making the operation of the reactor safer while, at the same time, the productivity is improved satisfactorily.

Acknowledgement

The financial support of the Embassy of France, Colfuturo and Universidad Nacional de Colombia is greatly acknowledged.

Nomenclature

C_{pj}	Specific heat of component j [J.K^{-1}.kg^{-1}]
I	Moles of initiator in the reactor [mol]
k_{fm}	Rate constant for chain transfer to monomer [m^3.mol^{-1}.s^{-1}]
k_{fp}	Rate constant for chain transfer to polymer [m^3.mol^{-1}.s^{-1}]
k_t	Termination rate constant [m^3.mol^{-1}.s^{-1}]
k_I	Overall initiation rate constant [s^{-1}]
M_M	Moles of monomer in the reactor [mol]
$\bar{M}_n$	Number average molecular weight [g.mol^{-1}]
$\bar{M}_w$	Weight average molecular weight [g.mol^{-1}]
M_t	Total moles of monomer fed to the reactor [mol]
MW_M	Monomer molecular weight [kg.mol^{-1}]
m_w	Mass of water in the reactor jacket [kg]
$\bar{n}$	Average number of radicals per particle [-]
q_I	Flow rate of initiator fed to the reactor [mol.s^{-1}]
q_M	Flow rate of monomer fed to the reactor [mol.s^{-1}]
$\mathcal{R}_{pol}$	Overall reaction rate [mol.s^{-1}]
T	Reactor temperature [K]
T_j	Jacket temperature [K]
U	Overall heat transfer coefficient [W.m^{-2}.K^{-1}]
V_{pol}	Total volume of polymer generated in the reaction [m^3]
V_w	Total volume of aqueous phase [m^3]
α	Probability of propagation [-]
ΔH_r	Heat of reaction [J.kg^{-1}]
λ_0	Total concentration of zeroth moment for growing chains [-]
μ_0	Concentration of zeroth moment for dead chains [-]
μ_1	Concentration of first moment for dead chains [-]

μ_2 Concentration of second moment for dead chains [-]
ϕ_S Solids content [-]
ρ_{pol} Polymer density [kg.m^{-3}]

References

Araújo, P., Giudici, R., 2003. Optimization of semicontinuous emulsion polymerization reactions by IDP procedure with variable time intervals. Comp. Chem. Engng 27, 1345–1360.

Arora, S., Gesthuisen, R., Engell, S., 2007. Model based operation of emulsion polymerization reactors with evaporative cooling: Application to vinyl acetate homopolymerization. Comp. Chem. Engng 31, 552–564.

Benyahia, B., Latifi, M. A., Fonteix, C., Pla, F., 2011. Multicriteria dynamic optimization of an emulsion copolymerization reactor. Comp. Chem. Engng 35, 2886–2895.

Biegler, L., 2007. An overview of simultaneous strategies for dynamic optimization. Chemical Engineering and Processing 46, 1043–1053.

Cervantes, A., Biegler, L. T., October 2008. Optimization strategies for dynamic systems, Encyclopedia of Optimization, Second Edition. Springer, pp. 216–227.

Chachuat, B., 2007. Nonlinear and Dynamic Optimization: From Theory to Practice.

Chylla, R. W., Haase, D. R., 1993. Temperature control of semibatch polymerization reactors. Comp. Chem. Engng 17, 257–264.

Corriou, J. P., 2004. Process Control - Theory and Applications. Springer Verlag, London, England.

Corriou, J. P., 2012. Commande des Procédés, 3rd Edition. Lavoisier, Tec. & Doc., Paris, France.

Gentric, C., Pla, F., Latifi, M. A., Corriou, J., 1999. Optimization and nonlinear control of a batch emulsion polymerization reactor. Chemical Engineering Journal 75, 31–46.

Gil, I. D., Vargas, J. C., Corriou, J. P., 2014. Nonlinear geometric temperature control of a vinyl acetate emulsion polymerization reactor. Ind. Eng. Chem. Res. 53, 7397–7408.

Graichen, K., Hagenmeyer, V., Zeitz, M., 2006. Feedforward control with online parameter estimation applied to the Chylla-Haase reactor benchmark. Journal of Process Control 16, 733–745.

Hvala, N., Aller, F., Miteva, T., Kukanja, D., 2011. Modelling, simulation and control of an industrial, semi-batch, emulsion-polymerization reactor. Comp. Chem. Engng 35, 2066–2080.

Ibrahim, W. H. B. W., Mujtaba, I. M., Alhamad, B. M., 2011. Optimisation of emulsion copolymerization of styrene and MMA in batch and semi-batch reactors. Chemical Product and Process Modeling 6, 1–18.

Jang, S. S., Yang, W. L., 1989. Dynamic optimization of batch emulsion polymerization of vinyl acetate - an orthogonal polynomial initiator policy. Chemical Engineering Science 44, 515–528.

Kameswaran, S., Biegler, L. T., 2006. Simultaneous dynamic optimization strategies: recent advances and challenges. Comp. Chem. Engng. 30, 1560–1575.

Paulen, R., Fikar, M., Latifi, M. A., 2010. Dynamic optimization of a hybrid system: emulsion polymerization reaction. Journal of Cybernetics and Informatics 9, 31–40.

Penlidis, A., 1986. Polymer reactor design, optimization and control in latex production technology. PhD thesis, McMaster University, Hamilton, Ontario.

Penlidis, A., MacGregor, J. F., Hamielec, A. E., 1985. Dynamic modeling of emulsion polymerization reactors. AIChE Journal 31, 881–889.

Sayer, C., Arzamendi, G., Asua, J. M., Lima, E. L., Pinto, J. C., 2001. Dynamic optimization of semicontinuous emulsion copolymerization reactions: composition and molecular weight distribution. Comp. Chem. Eng. 25, 839–849.

562 Silva, C. M., Biscaia Jr., E. C., 2004. Multi-objective dynamic optimization
563 of semi-batch polymerization processes. Macromol. Symp. 206, 291–306.

564 Vicente, M., Sayer, C., Leiza, J. R., Arzamendi, G., Lima, E. L., Pinto,
565 J. C., Asua, J. M., 2002. Dynamic optimization of non-linear emulsion
566 copolymerization systems. Open-loop control of composition and molecular
567 weight distribution. Chemical Engineering Journal 85, 339–349.